Toxicology and Applied Pharmacology 335 (2017) 1–5

Contents lists available at ScienceDirect

Toxicology and Applied Pharmacology

journal homepage: www.elsevier.com/locate/taap

Short Communication

Inhalation exposure to three-dimensional printer emissions stimulates acute hypertension and microvascular dysfunction

A.B. Stefaniak[b,c], R.F. LeBouf[c], M.G. Duling[c], J. Yi[a,c], A.B. Abukabda[a,b], C.R. McBride[a,b], T.R. Nurkiewicz[a,b,c,*]

[a] Department of Physiology, Pharmacology and Neuroscience, West Virginia University School of Medicine, Morgantown, WV, USA
[b] Toxicology Working Group, West Virginia University School of Medicine, Morgantown, WV, USA
[c] National Institute for Occupational Safety and Health, Morgantown, WV, USA

ARTICLE INFO

Keywords:
Ultrafine particle
Inhalation
Microcirculation
Endothelium
Hypertension

ABSTRACT

Fused deposition modeling (FDM™), or three-dimensional (3D) printing has become routine in industrial, occupational and domestic environments. We have recently reported that 3D printing emissions (3DPE) are complex mixtures, with a large ultrafine particulate matter component. Additionally, we and others have reported that inhalation of xenobiotic particles in this size range is associated with an array of cardiovascular dysfunctions. Sprague-Dawley rats were exposed to 3DPE aerosols via nose-only exposure for ~3 h. Twenty-four hours later, intravital microscopy was performed to assess microvascular function in the spinotrapezius muscle. Endothelium-dependent and -independent arteriolar dilation were stimulated by local microiontophoresis of acetylcholine (ACh) and sodium nitroprusside (SNP). At the time of experiments, animals exposed to 3DPE inhalation presented with a mean arterial pressure of 125 ± 4 mm Hg, and this was significantly higher than that for the sham-control group (94 ± 3 mm Hg). Consistent with this pressor response in the 3DPE group, was an elevation of ~12% in resting arteriolar tone. Endothelium-dependent arteriolar dilation was significantly impaired after 3DPE inhalation across all iontophoretic ejection currents (0–27 ± 15%, compared to sham-control: 15–120 ± 21%). Endothelium-independent dilation was not affected by 3DPE inhalation. These alterations in peripheral microvascular resistance and reactivity are consistent with elevations in arterial pressure that follow 3DPE inhalation. Future studies must identify the specific toxicants generated by FDM™ that drive this acute pressor response.

1. Introduction

Fused deposition modeling (FDM™) is a type of material extrusion three-dimensional (3D) printing technology in which a polymer filament is heated and extruded through a nozzle to create an object. We have previously characterized the aerosols generated and emitted during FDM™ 3D printing (Yi et al., 2016; Stefaniak et al., 2017). These studies have demonstrated that thermal decomposition of polymer filaments during 3D printer operation releases billions of ultrafine particles ($PM_{0.1}$, particles with at least one dimension < 100 nm) per minute, with emission rates being higher for acrylonitrile butadiene styrene (ABS) polymer compared to poly lactic acid (PLA) polymer. During thermal decomposition, numerous volatile organic chemicals (VOCs) are released into air, including aldehydes, ketones, alcohols, and aromatics (benzene, toluene, ethylbenzene, xylenes, and styrene). In addition to these primary emissions, some secondary reaction products were formed by the interaction of ozone with certain VOCs to produce carbonyl compounds.

$PM_{0.1}$ is generated largely from combustion-related processes (Kuwayama et al., 2013), and inhalation is the primary exposure route (Oberdorster et al., 1995). $PM_{0.1}$ inhalation has been positively associated with cardiovascular morbidity (Liu et al., 2013) and mortality (Su et al., 2015). Experimentally, these outcomes have been characterized as ischemia/reperfusion injury, conduction abnormalities, vascular dysfunction and hemostasis (Cascio et al., 2007; Courtois et al., 2008; Samet et al., 2009). We have documented that FDM™ 3D printing emissions (3DPE) are complex particulate aerosols with a significant fraction of particles in the ultrafine range (Yi et al., 2016). Therefore, it is reasonable to anticipate that alterations in cardiovascular function may follow 3DPE inhalation exposures.

Over the past decade, we have reported robust systemic microvascular dysfunction after inhalation of fine particulate matter

* Corresponding author at: Department of Physiology, Pharmacology and Neuroscience, 1 Medical Center Drive, Robert C. Byrd Health Sciences Center, West Virginia University, Morgantown, WV, 26506-9105, USA.
E-mail address: tnurkiewicz@hsc.wvu.edu (T.R. Nurkiewicz).

http://dx.doi.org/10.1016/j.taap.2017.09.016
Received 13 September 2017; Accepted 19 September 2017
Available online 21 September 2017
0041-008X/ © 2017 Published by Elsevier Inc.

(Nurkiewicz et al., 2004; Nurkiewicz et al., 2006) and nanoparticles (Nurkiewicz et al., 2008; Nurkiewicz et al., 2009). While all nanoparticles are not ultrafine PM, the two particles do share physical commonality in their defined sub 100 nm size. Cardiovascular function has not been assessed after 3DPE inhalation exposure. Therefore, we hypothesized that a similar biological response should follow 3DPE inhalation. However, these effects may not be implicitly similar as 3DPE are a more dynamic mixture of solids and gases, undergoing phase changes. Therefore, the purpose of this study was to initiate assessments of the acute cardiovascular and systemic microvascular consequences of 3DPE inhalation.

2. Methods

2.1. Animal model

All procedures and experiments in this study conformed to the National Institutes of Health (NIH) Guide for the Care and Use of Laboratory Animals (8th Edition) and were approved by the West Virginia University Animal Care and Use Committee. Male, Sprague-Dawley rats (7–8 weeks of age) were purchased from Hilltop Laboratories (Scottdale, PA), and housed in an AAALAC approved animal facility at the West Virginia University Health Sciences Center. All animals were maintained on a 12-hour light/dark cycle, provided food and water ad libitum, and acclimated for at least 72 h prior to training and/or use. Animals were then randomly assigned to either the Sham-Control (filtered air) or 3DPE inhalation exposure groups.

2.2. 3DPE generation and aerosol inhalation exposure

All rats were progressively trained daily for ~2 weeks prior to nose-only exposures. During these sessions, rats were placed in restraining tubes (Allay®, DSI, St. Paul, MN) initially for ~5 min, and progressively increased in 15–20 minute intervals for up to 4 h. Tubes were wrapped in red polyurethane sheets to reduce visual stress. At any point during training or exposure, if rats displayed distress, they were immediately removed. On experimental days, rats were placed in a nose-only exposure system (Inhalation Tower, DSI, St. Paul, MN) for 3–4 h. The stainless steel, nose-only exposure device is designed to accommodate up to 14 rodents. The tower has two levels of seven exposure ports, radially positioned around the aerosol delivery components of the system.

A desktop 3D printer (Replicator® 2×, MakerBot Industries, Brooklyn, NY) was placed in a 500 L stainless steel chamber. Black ABS is among the more common filaments used in 3D printing, and was used for all rat inhalation exposures herein. The printer was operated continuously during rat exposures. Emissions from the chamber were pumped into the nose-only exposure tower. Real-time and time-integrated aerosol sampling and monitoring instrumentation analyzed the emissions in the generation chamber and nose-only exposure tower as previously described (Yi et al., 2013). Briefly, 3DPE particle size distribution and mass concentration were measured continuously with a scanning mobility particle sizer (SMPS, TSI Inc., Shoreview, MN), and an electric low-pressure impactor (ELPI, Dekati, Ltd., Kangasala, Finland). The aerosol mass concentration was verified gravimetrically.

2.3. Intravital microscopy

At 24 h. post-exposure, rats were anesthetized with thiobutabarbital sodium (Inactin, 100 mg/kg, i.p.), placed on a heating plate, connected to a thermocouple probe to maintain a 37 °C rectal temperature with an Animal Temperature Controller (World Precision Instruments, Sarasota, Florida). The trachea was intubated to ensure a patent airway, and the right carotid artery was cannulated to measure arterial pressure. The right spinotrapezius muscle was then exteriorized for microscopic observation, leaving its innervation and all feed vessels intact. After exteriorization, the muscle was gently secured over an optical pedestal at its in situ length. The muscle was next enclosed in a tissue bath for transillumination and observation. Throughout the surgery and all experimental periods, the muscle was continuously superfused with an electrolyte solution (119 mM NaCl, 25 mM $NaHCO_3$, 6 mM KCl and 3.6 mM $CaCl_2$), warmed to 35 °C, and equilibrated with 95% N_2 – 5% CO_2 (pH = 7.35–7.40). Superfusate flow rate was maintained at 4–6 mL/min to minimize equilibration with atmospheric oxygen (Boegehold and Bohlen, 1988).

The animal preparation was then transferred to the stage of an intravital microscope, coupled to a CCD color video camera (BX51WI and DP71, respectively, Olympus, Tokyo, Japan). Observations were made with a 20× water immersion objective (final video image magnification = 1460×). One to three arterioles were studied per rat. Real-time images were displayed on a high-definition computer monitor and digitally captured for off-line analysis (Nurkiewicz et al., 2008, 2009). Arteriolar inner diameters were measured with Image-J software (National Institutes of Health, Bethesda, MD) calibrated with a stage micrometer.

2.4. Microiontophoresis

Micropipettes were custom fabricated with a Flaming/Brown Micropipette Puller (P-97, Sutter Instruments, Novato, CA). Aluminosilicate glass capillary tubes (A100-64-10, Sutter Instruments) were pulled to an inner diameter of 2–4 μm and subsequently double-beveled (BV-10, Sutter Instruments), as previously described (Nurkiewicz and Boegehold, 2004). Micropipettes were then backfilled with the muscarinic agonist acetylcholine (0.025 M; ACh), or the nitric oxide donor sodium nitroprusside (0.05 M; SNP). Backloaded pipettes were attached to a microelectrode holder with an indwelling Ag/AgCl wire that was connected to a Dual Microiontophoresis Current Programmer (SYS-260; World Precision Instruments, Sarasota, FL). The microelectrode holder was attached to a three-axis hydraulic micromanipulator, combined with a one-axis hydraulic micromanipulator (MMO-203, and MMO-220A respectively, Narishige, Tokyo, Japan) to enable four-dimensional controlled movements. The entire apparatus was mounted on a motorized stage platform (GMHB-BX, Gibraltar Industries, Buffalo, NY), adjacent to the animal preparation. Finally, an additional Ag wire was submerged in the intravital tissue bath to complete the electrical circuit. The micropipette was positioned with the tip within the arteriolar adventitial layer, slightly superior to the vessel wall to prevent accidental puncture associated with tissue movement and dilation. Holding currents of 200–500 nA were used to contain agonists in the micropipette during all control and recovery periods. Microiontophoretic ejection currents were randomly generated to evaluate endothelium-dependent dilation (ACh; 20, 40, and 100 nA), and endothelium-independent dilation (SNP; 5, 10 and 20 nA). At the end of all experiments, passive maximum arteriolar diameter was established by superfusing the tissue with 10^{-4} M adenosine (ADO).

2.5. Formulas, data and statistical analysis

Mean arterial pressure (MAP) was calculated as: MAP = diastolic pressure + (systolic pressure − diastolic pressure) / 3. Arteriolar diameter (D, μm) was sampled at 10-second intervals during all control and ejection periods. Resting vascular tone was calculated for each vessel as follows: Tone = $[(D_{pass} - D_c) / D_{pass}] \times 100$, where D_{pass} is passive diameter under ADO and D_c is the diameter measured during the control period (resting diameter). A tone of 100% represents complete vessel closure, and 0% represents the passive state. To evaluate arteriolar responsiveness between individual groups with subtle differences in resting diameter, arteriolar diameter was normalized. In this case, arteriolar diameter was expressed as a percent change from control and was calculated for each vessel as follows: Diameter (% change from control) = $[(D_{SS} - D_c) - 1 \times 100]$, where D_{SS} is the steady state

diameter achieved during ejection. All data are reported as means ± SE, where "N" represents the number of rats studied and "n" represents the number of arterioles evaluated. One to three microvessels were studied per rat. Statistical analysis was performed by commercially available software (Sigmaplot, Systat Software Inc., San Jose, CA). One-way repeated measures ANOVA was used to determine the effect of a treatment within a group, or differences among groups. Two-way repeated measures ANOVA was used to determine the effects of group, treatment and group-treatment interactions on measured variables. For all ANOVA procedures, the Student-Newman-Keuls method for post-hoc analysis was used to isolate pairwise differences among specific groups. Significance was assessed at the 95% confidence level ($P < 0.05$) for all tests.

3. Results

The 3DPE aerosol concentration in the nose-only exposure tower was 0.9 ± 0.1 mg/m^3. This concentration was verified by sampling multiple ports in different positions on the tower. The mean mobility diameter (SMPS) was 79 ± 9 nm, and the mean aerodynamic diameter (ELPI) was 70 ± 2 nm. These real-time aerosol measurements are consistent with those previously reported for black ABS filaments by our group (Yi et al., 2016; Stefaniak et al., 2017). The exposure duration was 180 ± 35 min. The calculated lung burden (dose) in the 3DPE inhalation group was 4.0 ± 0.4 μg. Rats in the Sham-Control group were placed in the Allay® restraint system, and connected to the nose-only exposure tower for a similar time, but only HEPA filtered air was passed through the system.

At the time of intravital microscopy experiments, there were no differences in age or body weight between the Sham-Control and 3DPE inhalation groups (Table 1). However, MAP was significantly elevated by ~28% after 3DPE inhalation. Heat rate was not different between the two groups (344 ± 13 vs 343 ± 15) for Sham-Control and 3DPE, respectively. Consistent with an increase in systemic pressure, arteriolar resting diameter was significantly smaller after 3DPE inhalation (Table 2). Because there was no structural effect on passive diameter, resting arteriolar tone was also significantly increased after 3DPE inhalation (Table 2).

Endothelium-dependent arteriolar dilation was significantly impaired after 3DPE inhalation (Fig. 1A). This was evident at the 40 and 100 nA ejection currents where arterioles in the Sham-Control group displayed dose-dependent responses to ACh iontophoresis, but arterioles in the 3DPE group did not. To account for subtle shifts in tone or peripheral resistance, the data were normalized as the percent change from control, and this relationship becomes more apparent (Fig. 1B).

Endothelium-independent arteriolar dilation was not altered after 3DPE inhalation (Fig. 2A). This was consistent at all ejection currents (5, 10 and 20 nA). To account for subtle shifts in tone or peripheral resistance, the data were also normalized as the percent change from control, but this did not reveal any significant effect (Fig. 2B).

4. Discussion

To our knowledge, these are the first assessments of cardiovascular function after 3DPE inhalation exposures. We report not only that MAP is significantly elevated after these exposures, but also that systemic microvascular dysfunction ensues. This latter observation manifests in the form of arteriolar vasoconstriction, or increased resting tone, and may be interpreted as an increase in peripheral resistance. Furthermore, microvascular relaxation, or endothelium-dependent arteriolar dilation is significantly impaired after 3DPE inhalation.

Perhaps the most important observation in this study is the MAP disturbance after 3DPE inhalation (Table 1). This is particularly striking as these direct measurements of arterial pressure were made under general anesthesia (Inactin). Arterial pressure is essentially the product of cardiac output and total peripheral resistance. Because cardiac output is the product of heart rate and stroke volume, we can derive: arterial pressure = (heart rate ∗ stroke volume) ∗ total peripheral resistance. Heart rate was not altered after 3DPE inhalation. Whereas, systemic arterioles were significantly constricted (elevated tone) after 3DPE inhalation (Table 2), and this directly contributes to an elevated peripheral resistance (Schmid-Schonbein et al., 1987). Therefore, our observation that MAP is increased after 3DPE inhalation, is due at least in part, to arteriolar vasoconstriction. Whether stroke volume is impacted must be determined via echocardiography in future experiments.

Arteriolar responsiveness to ACh iontophoresis was significantly impaired after 3DPE inhalation (Fig. 1). We have previously observed this type of dysfunction after pulmonary exposure to nanomaterials such as titanium dioxide (Nurkiewicz et al., 2011; Stapleton et al., 2015), cerium dioxide (Minarchick et al., 2013; Minarchick et al., 2015), and carbon nanotubes (Stapleton et al., 2012). However, single toxicant based studies do not accurately relate to the complexity of emissions generated by the 3D printing process. Fortunately, other groups have reported similar vascular consequences after exposure to complex mixtures of respirable PM and emission gases (Aragon et al., 2016). A lack of proper endothelium-dependent dilation in any microvascular bed results in the inability to adjust or maintain tissue perfusion with a variety of homeostatic processes (Pohl et al., 1994; Durand and Gutterman, 2013). While such microvasculopathy may be acutely tolerable or merely a protective mechanism, greater tissue function is ultimately compromised and chronic toxicity may elevate the risk of peripheral vascular disease (Frisbee et al., 2016).

The underlying toxicant(s) responsible for our observed hypertensive effect after 3DPE inhalation must be identified in future studies. We have directly measured mean arterial pressure in all our xenobiotic particle exposure/microvascular experiments since 2004. Despite the diversity of particle toxicants over those exposures, we have never detected a pressor response (acute hypertension). By deduction, we speculate that VOCs may be driving the acute hypertensive effect that follows 3DPE inhalation. VOC exposure has been associated with a host of pathologies, including hypertension (Nakhleh et al., 2017). Regarding our 3DPE exposures (black ABS), ethanol was one of the principal VOCs (Stefaniak et al., 2017). Interestingly, ethanol inhalation in rats has been shown to increase aortic tension/tone (Karanian and Salem, 1986), and stimulate an acute pressor response via alterations in vascular prostaglandin (Karanian et al., 1986) and catecholamine sensitivities (Karanian and Salem, 1988). Follow-up studies will explore if this possibility manifests itself at the microvascular level, and is indeed responsible for the pressor response that we report herein.

Table 1
Animal Characteristics at the time of intravital microscopy experiments. N = number of animals. Data are means ± SE.

Group	N	Age (days)	Weight (grams)	MAP (mm Hg)	Heart rate (beats/minute)
Sham-Control	8	58 ± 2	269 ± 16	94 ± 3	344 ± 13
3DPE inhalation	10	54 ± 3	273 ± 10	125 ± 4*	343 ± 15

* $P < 0.05$ vs Sham-Control group.

Table 2
Arteriolar Characteristics at the time of intravital microscopy experiments. n = number of arterioles. Data are means ± SE.

Group	n	D_{rest} (μm)	D_{pass} (μm)	Tone (%)
Sham-Control	19	46 ± 2	111 ± 5	58 ± 3
3DPE inhalation	19	38 ± 2*	114 ± 5	66 ± 2 *

* $P < 0.05$ vs Sham-Control group.

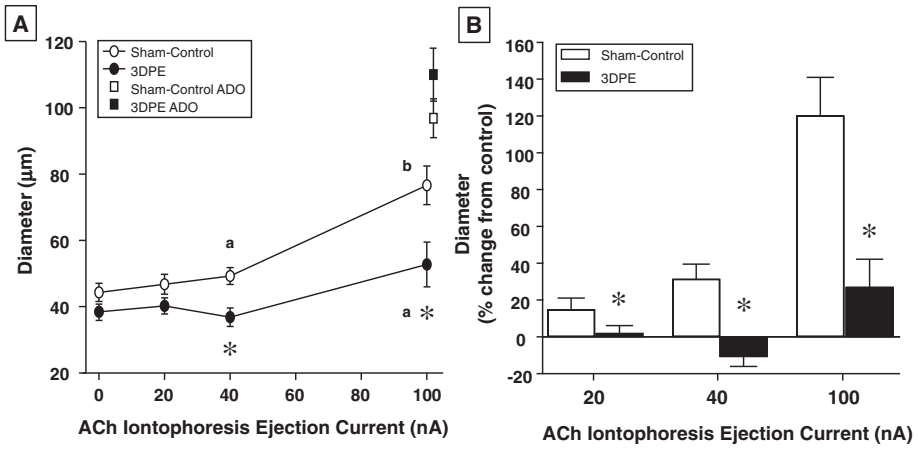

Fig. 1. Endothelium-dependent arteriolar dilation is impaired after 3DPE inhalation. Panel A: Arteriolar ACh responsiveness plotted in raw data form. Panel B: Because differences exist at specific points, the data are normalized as % change from control. Sham-Control group, n = 12; 3DPE group, n = 11. *, P < 0.05 vs Sham-Control at that ACh iontophoresis ejection current. a, P < 0.05 vs 0 nA response in group. b, P < 0.05 vs 40 nA response in group.

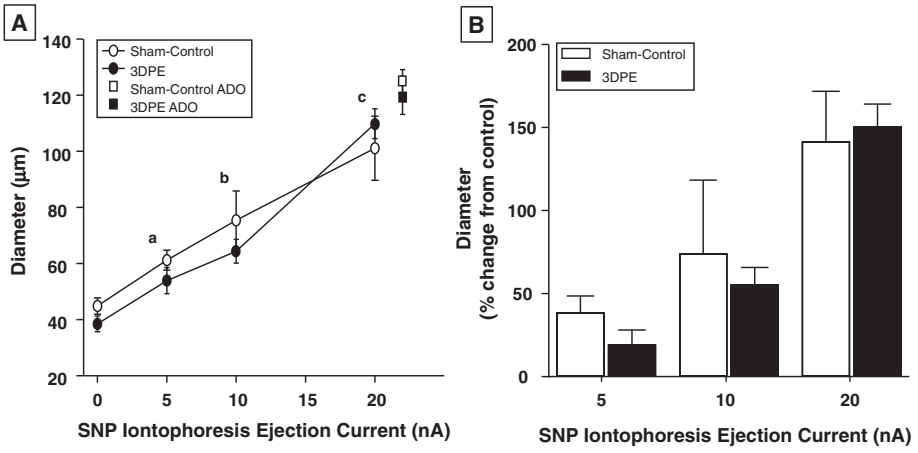

Fig. 2. Endothelium-independent arteriolar dilation is not impaired after 3DPE inhalation. Panel A: Arteriolar SNP responsiveness plotted in raw data form. Panel B: For consistency and comparison between figures, the data are normalized as % change from control. Sham-Control group, n = 7; 3DPE group, n = 8. a, P < 0.05 vs 0 nA response in group. b, P < 0.05 vs 5 nA response in group. c, P < 0.05 vs 10 nA response in group.

In summary, this is the first report that 3DPE inhalation is associated with an arterial pressor response, that is largely dependent on an increase in systemic microvascular resistance and impairments in endothelial reactivity. Given the complexity of cardiovascular homeostasis, future studies must assess if tissue profusion and/or cardiac function (e.g., stroke volume, ejection fraction) are compromised in this toxicity. Of equal importance will be to assess if exposure to other types of FDM™ 3D printing filaments results in similar cardiovascular outcomes.

5. Conclusion

The potential risk of 3DPE exposures could be reduced and/or avoided by proper engineering containment strategies and ventilation. This may be particularly important for sensitive populations such as those with preexisting cardiovascular disease.

Disclaimer

Mention of a specific product or company does not constitute endorsement by the Centers for Disease Control and Prevention. The findings and conclusions in this article are those of the authors and do not necessarily represent the views of the National Institute for Occupational Safety and Health.

Conflict of interests

The authors report no conflict of interest.

Acknowledgements

This work was supported by: NIHR01-ES015022 (TRN); NSF-1003907 (TRN), and DGE-1144676 (ABA); NIOSH-NORA927ZLDM (ABS), 63382 (JY), and 63392 (TRN).

References

Aragon, M.J., Chrobak, I., Brower, J., Roldan, L., Fredenburgh, L.E., McDonald, J.D., Campen, M.J., 2016. Inflammatory and vasoactive effects of serum following inhalation of varied complex mixtures. Cardiovasc. Toxicol. 16, 163–171.

Boegehold, M.A., Bohlen, H.G., 1988. Arteriolar diameter and tissue oxygen tension during muscle contraction in hypertensive rats. Hypertension 12, 184–191.

Cascio, W.E., Cozzi, E., Hazarika, S., Devlin, R.B., Henriksen, R.A., Lust, R.M., Van Scott, M.R., Wingard, C.J., 2007. Cardiac and vascular changes in mice after exposure to ultrafine particulate matter. Inhal. Toxicol. 19 (Suppl. 1), 67–73.

Courtois, A., Andujar, P., Ladeiro, Y., Baudrimont, I., Delannoy, E., Leblais, V., Begueret, H., Galland, M.A., Brochard, P., Marano, F., Marthan, R., Muller, B., 2008. Impairment of NO-dependent relaxation in intralobar pulmonary arteries: comparison of urban particulate matter and manufactured nanoparticles. Environ. Health Perspect. 116, 1294–1299.

Durand, M.J., Gutterman, D.D., 2013. Diversity in mechanisms of endothelium-dependent vasodilation in health and disease. Microcirculation 20, 239–247.

Frisbee, J.C., Butcher, J.T., Frisbee, S.J., Olfert, I.M., Chantler, P.D., Tabone, L.E., d'Audiffret, A.C., Shrader, C.D., Goodwill, A.G., Stapleton, P.A., Brooks, S.D., Brock, R.W., Lombard, J.H., 2016. Increased peripheral vascular disease risk progressively constrains perfusion adaptability in the skeletal muscle microcirculation. Am. J. Physiol. Heart Circ. Physiol. 310, H488–504.

Karanian, J.W., Salem Jr., N., 1986. Effects of acute and chronic ethanol exposure on the response of rat aorta to a thromboxane mimic, U46619. Alcohol. Clin. Exp. Res. 10, 171–176.

Karanian, J.W., Salem Jr., N., 1988. The effect of alcohol inhalation on the cardiovascular state of the rat. Adv. Alcohol Substance Abuse 7, 221–225.

Karanian, J.W., D'Souza, N.B., Salem Jr., N., 1986. The effect of chronic alcohol inhalation on blood pressure and the pressor response to noradrenaline and the thromboxane-mimic U46619. Life Sci. 39, 1245–1255.

Kuwayama, T., Ruehl, C.R., Kleeman, M.J., 2013. Daily trends and source apportionment of ultrafine particulate mass (PM0.1) over an annual cycle in a typical California city. Environ. Sci. Technol. 47, 13957–13966.

Liu, L., Breitner, S., Schneider, A., Cyrys, J., Bruske, I., Franck, U., Schlink, U., Marian Leitte, A., Herbarth, O., Wiedensohler, A., Wehner, B., Pan, X., Wichmann, H.E., Peters, A., 2013. Size-fractioned particulate air pollution and cardiovascular emergency room visits in Beijing, China. Environ. Res. 121, 52–63.

Minarchick, V.C., Stapleton, P.A., Porter, D.W., Wolfarth, M.G., Ciftyurek, E., Barger, M., Sabolsky, E.M., Nurkiewicz, T.R., 2013. Pulmonary cerium dioxide nanoparticle exposure differentially impairs coronary and mesenteric arteriolar reactivity. Cardiovasc. Toxicol.

Minarchick, V.C., Stapleton, P.A., Sabolsky, E.M., Nurkiewicz, T.R., 2015. Cerium dioxide nanoparticle exposure improves microvascular dysfunction and reduces oxidative stress in spontaneously hypertensive rats. Front. Physiol. 6, 339.

Nakhleh, M.K., Amal, H., Jeries, R., Broza, Y.Y., Aboud, M., Gharra, A., Ivgi, H., Khatib, S., Badarneh, S., Har-Shai, L., Glass-Marmor, L., Lejbkowicz, I., Miller, A., Badarny, S., Winer, R., Finberg, J., Cohen-Kaminsky, S., Perros, F., Montani, D., Girerd, B., Garcia, G., Simonneau, G., Nakhoul, F., Baram, S., Salim, R., Hakim, M., Gruber, M., Ronen, O., Marshak, T., Doweck, I., Nativ, O., Bahouth, Z., Shi, D.Y., Zhang, W., Hua, Q.L., Pan, Y.Y., Tao, L., Liu, H., Karban, A., Koifman, E., Rainis, T., Skapars, R., Sivins, A., Ancans, G., Liepniece-Karele, I., Kikuste, I., Lasina, I., Tolmanis, I., Johnson, D., Millstone, S.Z., Fulton, J., Wells, J.W., Wilf, L.H., Humbert, M., Leja, M., Peled, N., Haick, H., 2017. Diagnosis and classification of 17 diseases from 1404 subjects via pattern analysis of exhaled molecules. ACS Nano 11, 112–125.

Nurkiewicz, T.R., Boegehold, M.A., 2004. Calcium-independent release of endothelial nitric oxide in the arteriolar network: onset during rapid juvenile growth. Microcirculation 11, 453–462.

Nurkiewicz, T.R., Porter, D.W., Barger, M., Castranova, V., Boegehold, M.A., 2004. Particulate matter exposure impairs systemic microvascular endothelium-dependent dilation. Environ. Health Perspect. 112, 1299–1306.

Nurkiewicz, T.R., Porter, D.W., Barger, M., Millecchia, L., Rao, K.M., Marvar, P.J., Hubbs, A.F., Castranova, V., Boegehold, M.A., 2006. Systemic microvascular dysfunction and inflammation after pulmonary particulate matter exposure. Environ. Health Perspect 114, 412–419.

Nurkiewicz, T.R., Porter, D.W., Hubbs, A.F., Cumpston, J.L., Chen, B.T., Frazer, D.G., Castranova, V., 2008. Nanoparticle inhalation augments particle-dependent systemic microvascular dysfunction. Part Fibre. Toxicol 5 (1), 12.

Nurkiewicz, T.R., Porter, D.W., Hubbs, A.F., Stone, S., Chen, B.T., Frazer, D.G., Boegehold, M.A., Castranova, V., 2009. Pulmonary nanoparticle exposure disrupts systemic microvascular nitric oxide signaling. Toxicol. Sci. 110, 191–203.

Nurkiewicz, T.R., Porter, D.W., Hubbs, A.F., Stone, S., Moseley, A.M., Cumpston, J.L., Goodwill, A.G., Frisbee, S.J., Perrotta, P.L., Brock, R.W., Frisbee, J.C., Boegehold, M.A., Frazer, D.G., Chen, B.T., Castranova, V., 2011. Pulmonary particulate matter and systemic microvascular dysfunction. Res. Rep. Health Eff. Inst 3–48.

Oberdorster, G., Gelein, R.M., Ferin, J., Weiss, B., 1995. Association of particulate air pollution and acute mortality: involvement of ultrafine particles? Inhal. Toxicol. 7, 111–124.

Pohl, U., Lamontagne, D., Bassenge, E., Busse, R., 1994. Attenuation of coronary autoregulation in the isolated rabbit heart by endothelium derived nitric oxide. Cardiovasc. Res. 28, 414–419.

Samet, J.M., Rappold, A., Graff, D., Cascio, W.E., Berntsen, J.H., Huang, Y.C., Herbst, M., Bassett, M., Montilla, T., Hazucha, M.J., Bromberg, P.A., Devlin, R.B., 2009. Concentrated ambient ultrafine particle exposure induces cardiac changes in young healthy volunteers. Am. J. Respir. Crit. Care Med. 179, 1034–1042.

Schmid-Schonbein, G.W., Zweifach, B.W., Delano, F.A., Chen, P.C., 1987. Microvascular tone in a skeletal muscle of spontaneously hypertensive rats. Hypertension 9, 164–171.

Stapleton, P.A., Minarchick, V.C., Cumpston, A.M., McKinney, W., Chen, B.T., Sager, T.M., Frazer, D.G., Mercer, R.R., Scabilloni, J., Andrew, M.E., Castranova, V., Nurkiewicz, T.R., 2012. Impairment of coronary arteriolar endothelium-dependent dilation after multi-walled carbon nanotube inhalation: a time-course study. Int. J. Mol. Sci. 13, 13781–13803.

Stapleton, P.A., McBride, C.R., Yi, J., Nurkiewicz, T.R., 2015. Uterine microvascular sensitivity to nanomaterial inhalation: an in vivo assessment. Toxicol. Appl. Pharmacol. 288, 420–428.

Stefaniak, A.B., LeBouf, R.F., Yi, J., Ham, J., Nurkewicz, T., Schwegler-Berry, D.E., Chen, B.T., Wells, J.R., Duling, M.G., Lawrence, R.B., Martin Jr., S.B., Johnson, A.R., Virji, M.A., 2017. Characterization of chemical contaminants generated by a desktop fused deposition modeling 3-dimensional printer. J. Occup. Environ. Hyg. 14, 540–550.

Su, C., Hampel, R., Franck, U., Wiedensohler, A., Cyrys, J., Pan, X., Wichmann, H.E., Peters, A., Schneider, A., Breitner, S., 2015. Assessing responses of cardiovascular mortality to particulate matter air pollution for pre-, during- and post-2008 Olympics periods. Environ. Res. 142, 112–122.

Yi, J., Chen, B.T., Schwegler-Berry, D., Frazer, D., Castranova, V., McBride, C., Knuckles, T.L., Stapleton, P.A., Minarchick, V.C., Nurkiewicz, T.R., 2013. Whole-body nanoparticle aerosol inhalation exposures. J. Vis. Exp. e50263.

Yi, J., LeBouf, R.F., Duling, M.G., Nurkiewicz, T., Chen, B.T., Schwegler-Berry, D., Virji, M.A., Stefaniak, A.B., 2016. Emission of particulate matter from a desktop three-dimensional (3D) printer. J. Toxicol. Environ. Health A 79, 453–465.